

Unsteady Unified Hypersonic/Supersonic Method for Aeroelastic Applications Including Wave/Shock Interaction

Frank R. Chavez*

University of Maryland, College Park, Maryland 20742
and

D. D. Liu†

Arizona State University, Tempe, Arizona 85287

A unified unsteady hypersonic/supersonic method using perturbed Euler characteristics (PEC) has been developed for the treatment of stability derivatives and panel flutter of wedgelike profiles. The present PEC method is valid for all supersonic Mach numbers, ranging from the low supersonic shock-attached limit to the Newtonian limit, in the complete frequency range, and for arbitrary body thickness so long as the bow shock remains attached to the body apex. The unsteady lifts, moments, and stability derivatives for oscillating wedge profiles, an oscillating leading-edge flap, and the related panel flutter problem are studied. Our computed results are found to differ with those of piston theory and linear potential theory in their invalid regions as expected. The essential feature of the PEC method lies in that it can fully account for the unsteady Mach wave/shock wave interaction and, hence, the rotationality and thickness effects. In view of its exactness, in terms of the characteristic formulation, and its ease of application, the present (PEC) method should be a promising method for panel flutter applications to hypersonic vehicles such as NASP.

Nomenclature

$C_{m\theta}$	= stiffness moment
$C_{m\dot{\theta}}$	= damping moment
c	= wedge chord length
H	= wedge surface shape function
i	= $\sqrt{-1}$
k	= reduced frequency, $\omega c/U_0$
M_0	= aft-shock mean flow Mach number
M_∞	= freestream Mach number
P	= unsteady perturbation pressure
P_0	= aft-shock mean flow pressure
P_∞	= freestream pressure
Q	= unsteady shock shape function, q/c
t	= nondimensional time, $\bar{t}U_0/c$
U	= unsteady x -axis perturbation velocity
U_0	= aft-shock mean flow velocity
V	= unsteady y -axis perturbation velocity
(x, y)	= nondimensional coordinates, $(\bar{x}/c, \bar{y}/c)$
x_0	= pitch axis location (nondimensional)
α	= angle of attack
β_0	= $\sqrt{M_0^2 - 1}$
γ	= ratio of specific heats
ε	= unsteady amplitude parameter
θ	= flow deflection angle
(ξ, η)	= characteristic coordinates
τ	= semiwedge angle
ω	= circular frequency

Introduction

ADVANCED configurations such as the National Aerospace Plane (NASP) (or X-30) are designed to operate at a cruising speed of $M_\infty = 15 \sim 20$, which corresponds to a dynamic pressure

around 2000 psf at an altitude of 120,000 ft. In this hypersonic/supersonic flight regime, not only will the attached unsteady shock wave cast a significant influence on the surface pressure distribution, but it will also, in turn, affect the vehicle's dynamic stability and the structural instability due to surface panel flutter under the high dynamic pressure environment. For aeroelastic applications, available methods to account for the unsteady body motion and shock wave interaction in the full frequency domain are lacking. Current computational fluid dynamic (CFD) methods associated with this type of problem mostly emphasize the flowfield details for aerodynamic inlet design, e.g., Ref. 1. For aeroelastic applications such as panel flutter they are too computationally expensive to be a practical engineering tool. Therefore, a more efficient unsteady hypersonic/supersonic method for aeroelastic applications is warranted.

The objective of the present work is twofold. First, a review is provided for existing methods in the treatment of unsteady-flow problems in this regime, notably piston theory² among others. Second, a perturbed Euler characteristics (PEC) method has been developed, and its computed results are presented here showing its superiority to the existing methods in terms of its accuracy and ease of application. In fact, the present PEC method is valid for all Mach numbers, ranging from the low supersonic shock-attached limit to the Newtonian limit, in the complete frequency range, and for arbitrary body thickness. The major thrust of the PEC method is that it fully accounts for the effect of unsteady Mach wave/shock wave interaction in the aforementioned Mach number and frequency ranges. The PEC method should be considered as an Euler approximation to the hypersonic flow. Therefore, it imposes no restriction on the value for the ratio of specific heats γ , except that it is not applicable to flow with dissociation and ionization effects.

Hypersonic/supersonic panel flutter analysis usually adopts piston theory, originally put forth by Hayes³ and Lighthill² and further extended by Ashley and Zartarian.⁴ In the high-Mach-number range, $M_\infty \gg 1$, Lighthill stated that piston theory is valid under the following assumptions:

$$M\delta < 1 \text{ and } Mk\varepsilon < 1$$

where δ is the maximum slope of the surface deflection. Landahl et al.⁵ also showed that piston theory is valid if any one of the following conditions holds:

$$M^2 \gg 1, \quad kM^2 \gg 1, \quad \text{or} \quad k^2M^2 \gg 1$$

Presented as Paper 93-1317 at the AIAA/ASME/ASCE/AHS/ASC 34th Structures, Structural Dynamics, and Materials Conference, La Jolla, CA, April 19–22, 1993; received July 8, 1993; revision received Sept. 7, 1994; accepted for publication Sept. 7, 1994. Copyright ©1994 by Frank R. Chavez and D. D. Liu. Published by the American Institute of Aeronautics and Astronautics, Inc. with permission.

*Doctoral Candidate, Department of Aerospace Engineering. Student Member AIAA.

†Professor of Engineering, Department of Mechanical and Aerospace Engineering. Member AIAA.

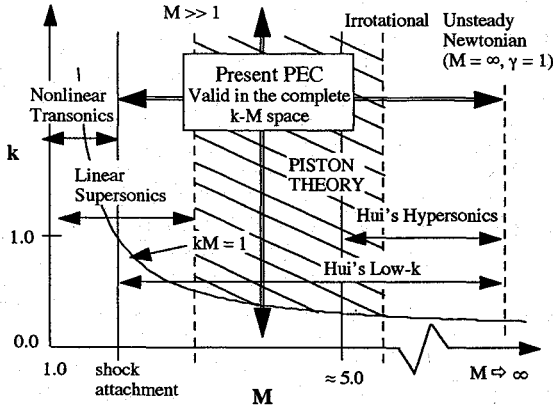


Fig. 1 M - k diagram illustrating various limits for hypersonic supersonic flow.

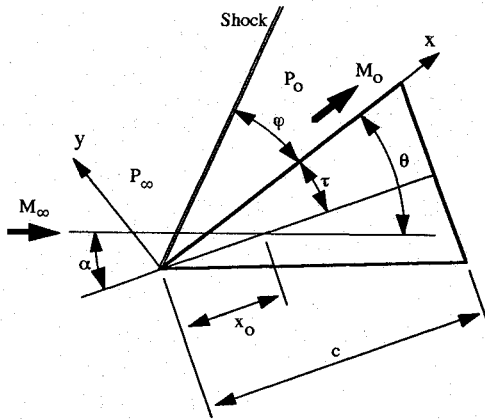


Fig. 2 Oscillating wedge with attached bow shock showing notation.

Although piston theory has demonstrated its ease of applicability to a wide class of practical configurations, including the body thickness effect, the valid flow region remains to be quantitatively defined. As shown in the M - k diagram of Fig. 1, the piston theory, for large values of the reduced frequency, is restricted to the low-supersonic-Mach-number range, and it does not approach the hypersonic Newtonian limit either. Furthermore, the application of piston theory is somewhat arbitrary. In recent years, it was reported that if the local Mach number (for curved profiles) or the aft-shock Mach number (for wedgelike profiles) is used in place of the freestream Mach number in the piston theory formula, improved results usually could be achieved (e.g., Refs. 6 and 7). However, such a practice may work for some cases, but it has little theoretical foundation.

For the problem of an oscillating wedge in hypersonic/supersonic flow, more rigorous approaches using Euler perturbation schemes for an unsteady flow formulation are due to Carrier,⁸ Van Dyke,⁹ McIntosh,⁶ and Hui.^{10,11} Carrier's approach splits the velocity field into a velocity potential component and a vorticity vector component. He was able to somewhat justify decoupling their governing equations, which amounts to a further approximation in the flow rotationality. Van Dyke extended Carrier's solution to allow for a general pitch axis location and presented a low-frequency analytical solution. McIntosh, on the other hand, formally generalized Van Dyke's hypersonic small disturbance theory¹² to unsteady flow over a thin wedge, which approaches the double limits, in M_∞ and γ , of Newtonian flow as expected.

Based on his exact linearized perturbed Euler formulation, Hui obtained two exact analytical solutions for the oscillating wedge problem.^{10,11} One is the exact solution of the low-frequency formulation,¹⁰ and the other is the exact solution of the hypersonic general-frequency approximation.¹¹ However, an exact analytical solution of the unified hypersonic/supersonic flow in the full-frequency domain remains unavailable.

The present PEC method attempts to solve the perturbed Euler equations, based on Hui's exact formulation,¹¹ by means of a method

of characteristics. As an initial-value problem, the PEC computational scheme starts from the wedge apex and marches on to the region bounded by the mean position of the attached shock wave and that of the wedge surface.

Consider the wedge profile as shown in Fig. 2, where φ denotes the angle measured from the mean surface of the wedge to that of the shock. Since the present PEC method can compute the flow over any compression surface, the mean flow patterns depend only on the freestream Mach number and θ ; therefore, it can handle any asymmetric body with or without mounted panels so long as both surfaces have shock waves attached to the wedge apex.

Analysis

Problem Formulation

Consider an oscillating wedge with attached shock wave as shown in Fig. 3. Based on the linear perturbation of small amplitude, the solution of the Euler equations is sought in the following form; i.e.,

$$\begin{aligned}\bar{P} &= P_0[1 + \varepsilon \gamma M_0^2 P(x, y)e^{ikt} + \mathcal{O}(\varepsilon^2)] \\ \bar{\rho} &= \rho_0[1 + \varepsilon \rho(x, y)e^{ikt} + \mathcal{O}(\varepsilon^2)] \\ \bar{U} &= U_0[1 + \varepsilon U(x, y)e^{ikt} + \mathcal{O}(\varepsilon^2)] \\ \bar{V} &= U_0[\varepsilon V(x, y)e^{ikt} + \mathcal{O}(\varepsilon^2)]\end{aligned}\quad (1)$$

where ρ_0 is the steady mean flow density behind the shock, and ρ is the perturbed density in the x and y directions.

Substituting Eqs. (1) into the Euler equations yields the linearized equations,

$$\begin{aligned}M_0^2(P_x + ikP) + U_x + V_y &= 0 \\ U_x + ikU + P_x &= 0 \\ V_x + ikV + P_y &= 0\end{aligned}\quad (2)$$

Equations (2) can be combined to yield a second-order equation for the pressure; i.e.,

$$\beta_0^2 P_{xx} - P_{yy} + i2kM_0^2 P_x - k^2 M_0^2 P = 0 \quad (3)$$

which is the acoustic equation for P . In passing, we note that Eq. (3) is identical to the governing equation for the linearized velocity potential (linear theory) with the freestream Mach number M_∞ replaced with the aft-shock Mach number M_0 .

The generalized unsteady flow tangency condition is to be satisfied on the wedge surface as shown in Fig. 3; i.e.,

$$\frac{DS}{Dt} = 0 \quad (4)$$

on

$$S = y - \varepsilon h(x, t) = 0 \quad (5)$$

where $h(x, t)$ represents the unsteady wedge surface motion. If the wedge motion is assumed harmonic with small amplitude ε , Eq. (4) can be simplified to yield the nondimensional tangency condition on the wedge surface, on $y = 0$,

$$V(x, 0) = H_x + ikH \quad (6)$$

where $h(x, t) = H(x)e^{ikt}$.

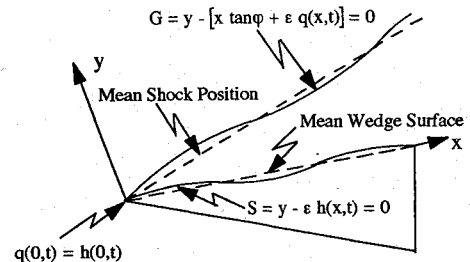


Fig. 3 Oscillating wedge with unsteady shock and wedge surface boundaries.

The unsteady motion of the shock is described by the following equation,

$$G = y - [x \tan \varphi + \varepsilon q(x, t)] = 0 \quad (7)$$

where $q(x, t) = Q(x)e^{ikt}$ represents the unsteady shock motion. Substituting Eqs. (1) and (7) into the Rankine-Hugoniot conditions yields Hui's linearized shock condition; i.e., on $y = x \tan \varphi$,

$$\begin{aligned} V(x, x \tan \varphi) &= A Q_x + ik B Q \\ P(x, x \tan \varphi) &= C Q_x + ik D Q \\ U(x, x \tan \varphi) &= E Q_x + ik F Q \end{aligned} \quad (8)$$

where the constant coefficients A , B , C , D , E , and F can be found in Ref. 10.

At the apex of the wedge, the shock is to be attached at all times, which amounts to the shock attachment condition, at $x = 0$,

$$Q(0) = H(0) \quad (9)$$

Furthermore, the apex condition also imposes the condition that the downwash velocity on the wedge surface and on the shock should yield the same value at the apex, at $x = 0$,

$$V(x, x \tan \varphi) = V(x, 0) \quad (10)$$

This additional apex condition provides the initial shock slope.

Perturbed Euler Characteristics (PEC)

Since the present formulation is a linearized one, it is plausible to adopt a linear characteristics approach based on the perturbed Euler equations, Eqs. (2) and (3). From Eq. (3), the characteristic directions are determined:

$$\left(\frac{dy}{dx} \right)_{\eta, \xi} = \pm \frac{1}{\beta_0} \quad (11)$$

Equation (11) can be integrated to give

$$\begin{aligned} \xi &= x + \beta_0 y \\ \eta &= x - \beta_0 y \end{aligned} \quad (12)$$

Based on the characteristic coordinates of Eqs. (12), the perturbed Euler equations, Eqs. (2) and (3), can be transformed accordingly. Hence, one obtains

Along constant η :

$$\beta_0^2 \frac{dP}{d\xi} + \beta_0 \frac{dV}{d\xi} + ik \frac{1}{2} (M_0^2 P + \beta_0 V - U) = 0 \quad (13)$$

Along constant ξ :

$$\beta_0^2 \frac{dP}{d\eta} - \beta_0 \frac{dV}{d\eta} + ik \frac{1}{2} (M_0^2 P - \beta_0 V - U) = 0 \quad (14)$$

The canonical form of the acoustic pressure equation becomes

$$4\beta_0^2 P_{\xi\eta} - i2kM_0^2 (P_\xi + P_\eta) - k^2 M_0^2 P = 0 \quad (15)$$

Method of Solution

A finite difference scheme is proposed to solve for the PEC equations on the characteristic mesh, as shown in Fig. 4. The figure depicts the constant ξ and η characteristics along which the equations governing the dependent variables are to be discretized. Equation (13), which governs the flow along constant η characteristics, will be applied at the midpoint of the characteristic connecting points C and D. A central-difference scheme yields the following discretized version of Eq. (13):

$$\begin{aligned} \beta_0^2 P^C + \beta_0 V^C + ik \frac{\Delta \xi}{4} (M_0^2 P^C + \beta_0 V^C - U^C) \\ = \beta_0^2 P^D + \beta_0 V^D - ik \frac{\Delta \xi}{4} (M_0^2 P^D + \beta_0 V^D - U^D) \end{aligned} \quad (16)$$

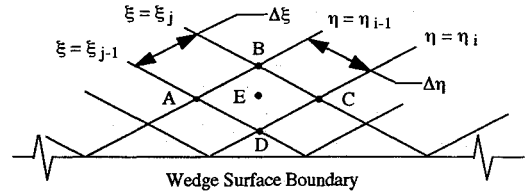


Fig. 4 Characteristic mesh on which the finite difference procedure is applied.

Equation (14), which governs the flow along constant ξ characteristics, will be applied at the midpoint of the characteristic connecting points B and C. Lastly, Eq. (15), which governs the pressure, will be applied at point E, the centroid of the finite mesh bounded by the points A, B, C, and D. A central-difference scheme is also used to discretize these two equations.

Applications

The PEC method is now applied to three typical cases for aeroelastic applications. These include a rigid wedge in pitching motion, leading-edge flap oscillation, and panel flutter, all including the unsteady Mach wave/shock wave interaction.

The total pressure coefficient \bar{C}_p can be expressed in terms of ε as

$$\bar{C}_p = C_{p0} + \varepsilon C_p e^{ikt} \quad (17)$$

where C_{p0} and C_p are, respectively, the pressure coefficients for the steady mean flow and for the unsteady perturbed flow,

$$C_{p0} = \frac{[(P_0/P_\infty) - 1]}{\frac{1}{2} \gamma M_\infty^2}, \quad C_p = 2 \left(\frac{M_0}{M_\infty} \right)^2 \left(\frac{P_0}{P_\infty} \right) P \quad (18)$$

In terms of the unsteady pressure coefficient C_p , the lift and moment coefficients are defined as

$$C_l = -2 \int_0^1 C_p dx, \quad C_m = 2 \int_0^1 C_p \left(x_0 - \frac{x}{\cos^2 \tau} \right) dx \quad (19)$$

Finally, the stiffness and damping moments $C_{m\theta}$ and $C_{m\dot{\theta}}$ are defined as

$$C_{m\theta} = \text{Re}(C_m), \quad C_{m\dot{\theta}} = \frac{\text{Im}(C_m)}{k} \quad (20)$$

Rigid Wedge in Pitching Motion

Verification with Hui's Theory

The hypersonic case presented in Fig. 5 is for a low reduced frequency, $k = 0.1$, and a high Mach number, $M_\infty = 20.0$. As expected, the PEC and Hui's hypersonic approximate method¹¹ agree quite well for the in- and out-of-phase pressure solution. From the figure, it is seen that the out-of-phase pressure solutions as calculated by the PEC and Hui's unified theory¹⁰ (low- k approximation) are nearly indistinguishable. The discrepancy in Hui's low-frequency in-phase pressure solution is due to neglecting the higher order terms in the frequency expansion. At a given moderate supersonic Mach number and a high reduced-frequency value, neither of Hui's solutions is expected to give accurate results. This is indeed the case that is shown in Fig. 6, where at a high reduced-frequency value of 5.0 and at Mach number 3.0, the effect of frequency as calculated by the PEC method is apparent.

Effect of Unsteady Wave/Shock Interaction

The pressure and unsteady shock shape showing the effect of the Mach wave/shock wave interaction at different instants of time during one cycle of the pitching motion of a wedge is presented in Fig. 7, at $M_\infty = 1.5$ and $k = 2.4$. It is seen that at a lower Mach number (Fig. 7) the pressure disturbances are wavy, whereas at a higher Mach number of $M_\infty = 3.0$ (Fig. 8), the waviness disappears. At $M_\infty = 1.5$ where the aft-shock Mach wave angle is larger ($\mu_0 = 65^\circ$) than the shock angle, multiple reflections of the Mach waves from the shock imparts upon and rebounds from the wedge surface.

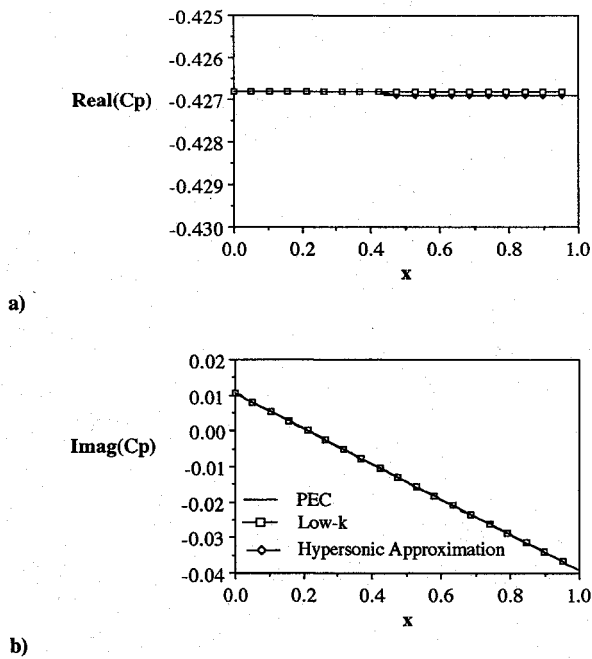


Fig. 5 Comparison of in-phase and out-of-phase pressure distribution over an oscillating wedge at $M_\infty = 20.0$ and $k = 0.1$ with pitch axis at $x_0 = 0.25$ (5-deg semiwedge angle).

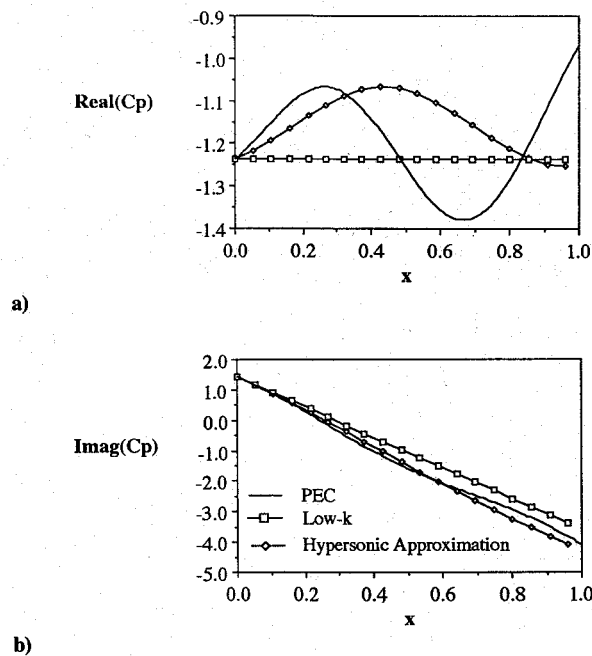


Fig. 6 Comparison of in-phase and out-of-phase pressure distribution over an oscillating wedge at $M_\infty = 3.0$ and $k = 5.0$ with pitch axis at $x_0 = 0.25$ (10-deg semiwedge angle).

This is not the case for $M_\infty = 3.0$ as the aft-shock Mach wave angle is smaller ($\mu_0 = 24$ deg) than the shock angle. Hence, Fig. 7 exhibits a strong (wave/shock) interaction.

Comparison with Linear Theory

Comparisons of results between those computed by the PEC method, piston theory,² and linear (potential) theory¹³ are presented in Figs. 9 and 10, which are the in- and out-of-phase pressure counterparts of Figs. 7 and 8. For these and subsequent results, the piston theory is applied to the freestream flow conditions and is third order in thickness. Since linear theory can account for the upstream influence, the superiority of the PEC solution over the linear theory solution lies mainly in that the former includes the effects of

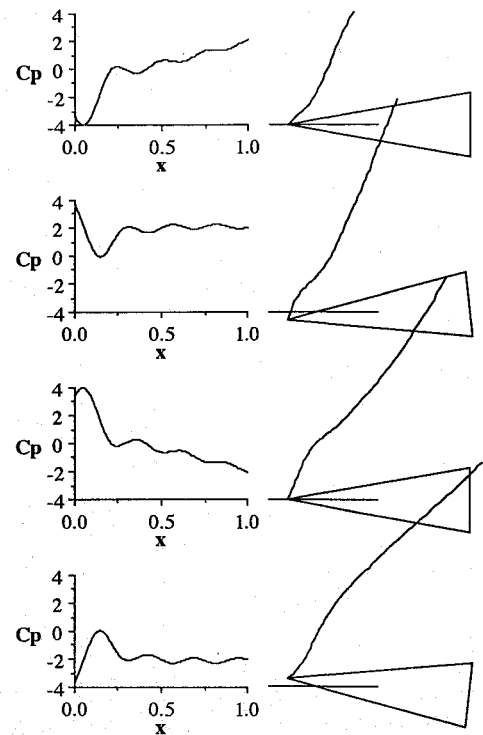


Fig. 7 Time-dependent pressure distribution over an oscillating wedge during one cycle of oscillation at $M_\infty = 1.5$ and $k = 2.4$ with pitch axis at $x_0 = 0.5$ (10-deg semiwedge angle).

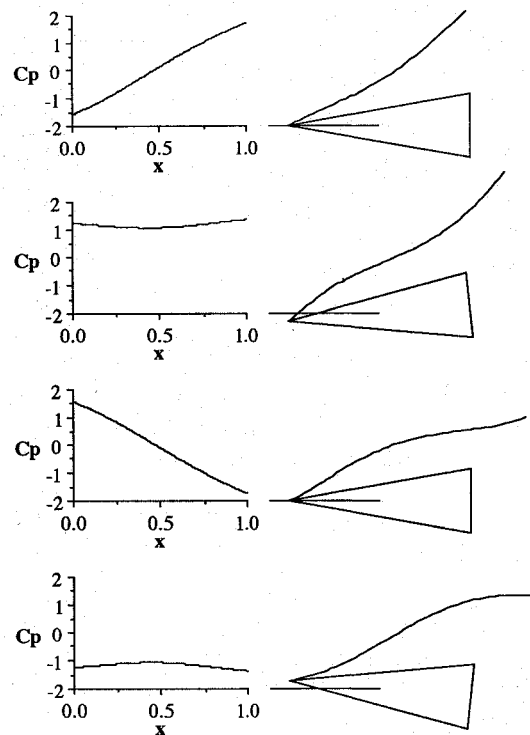
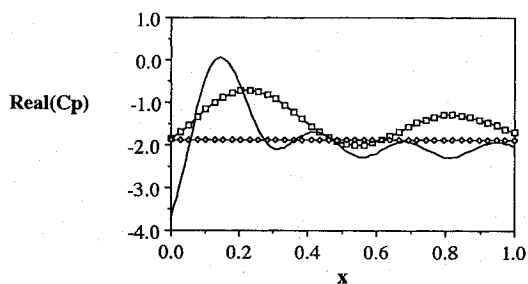
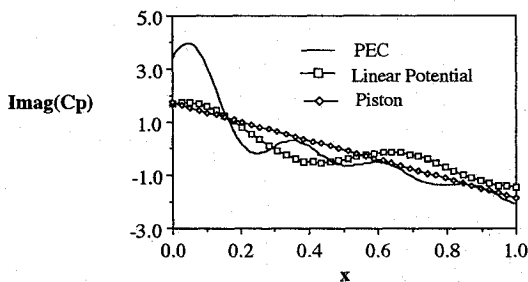


Fig. 8 Time-dependent pressure distribution over an oscillating wedge during one cycle of oscillation at $M_\infty = 3.0$ and $k = 2.77$ with pitch axis at $x_0 = 0.5$ (10-deg semi wedge angle).

rotationality, unsteady shock motion, and thickness. The superiority of the PEC solution over the piston theory solution lies in that the latter fails to include the effects of flow rotationality and the upstream influence. These differences in theory are clearly shown in the considerable departures between the computed results. For the low-Mach-number case of Fig. 9, both piston theory and linear theory fail to capture the large pressure peak near the apex and the pressure waviness that are due to the strong unsteady Mach

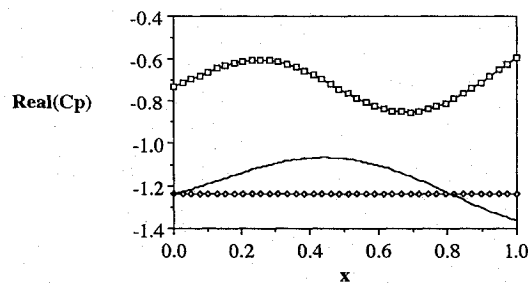


a)

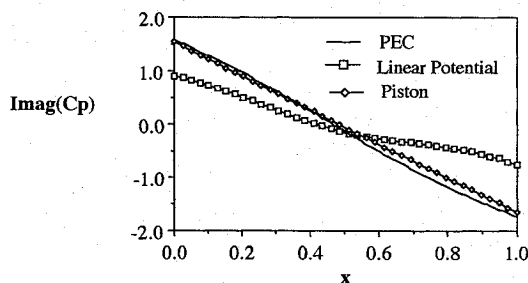


b)

Fig. 9 Comparison of in-phase and out-of-phase pressure distribution over an oscillating wedge at $M_\infty = 1.5$ and $k = 2.4$ with pitch axis at $x_0 = 0.5$ (10-deg semiwedge angle).



a)



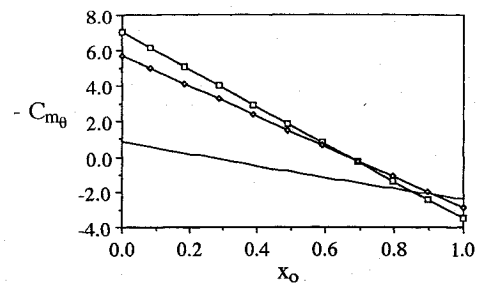
b)

Fig. 10 Comparison of in-phase and out-of-phase pressure distribution over an oscillating wedge at $M_\infty = 3.0$ and $k = 2.77$ with pitch axis at $x_0 = 0.5$ (10-deg semiwedge angle).

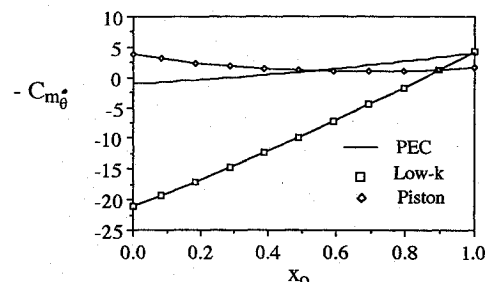
wave/shock wave interaction at the apex and over the surface. Although Fig. 10 confirms that mild Mach wave/shock interaction exists in the in- and out-of-phase pressures for the higher Mach number, their departures from results of piston theory and linear theory are, nevertheless, apparent.

Stability Derivatives

The effect of pitch axis location on the stiffness and damping-in-pitch moments computed from the present PEC method, piston theory,² and Hui's unified low- k ¹⁰ solution are presented in Figs. 11 and 12 for a 30 deg semiwedge angle at $k = 0.5$ and $M_\infty = 2.6$, which is just above the shock attachment limit, and at $M_\infty = 5.0$, respectively. For the low-Mach-number case of

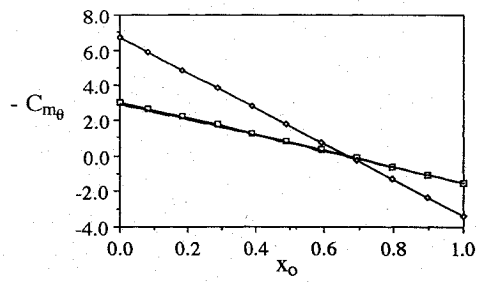


a)

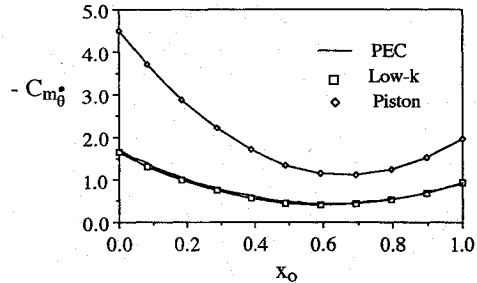


b)

Fig. 11 Effect of pitch axis location on the aerodynamic stiffness and damping derivatives for an oscillating wedge at $M_\infty = 2.6$ and $k = 0.5$ (30-deg semiwedge angle).



a)



b)

Fig. 12 Effect of pitch axis location on the aerodynamic stiffness and damping derivatives for an oscillating wedge at $M_\infty = 5.0$ and $k = 0.5$ (30-deg semiwedge angle).

Fig. 11, piston theory predicts a stable pitch damping derivative for all pitch axis locations, whereas the PEC solution predicts an unstable pitch damping derivative over a range of pitch axis locations. Concurrent with McIntosh's finding in Ref. 6, piston theory is shown to provide excessive damping for the cases considered. In fact, as measured by the PEC results at a moderate reduced frequency such as $k = 0.5$, it is seen that the predicted damping moments of piston theory tend to be nonconservative, whereas those of Hui's unified low- k theory tend to be conservative. At a high Mach number, such as $M_\infty = 5.0$ of Fig. 12, piston theory results seem to yield considerable discrepancy with others; this is expected as Lighthill's postulate, that $M\delta < 1$, ceases to be applicable in this case.

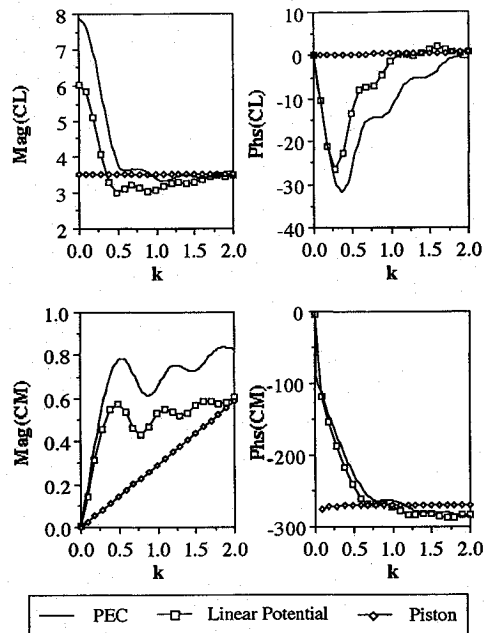


Fig. 13 Effect of frequency on the aerodynamic lift and moment for an oscillating wedge at $M_\infty = 1.2$ with pitch axis at $x_0 = 0.5$ (2-deg semiwedge angle).

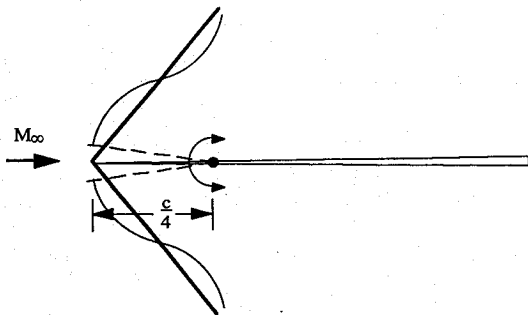


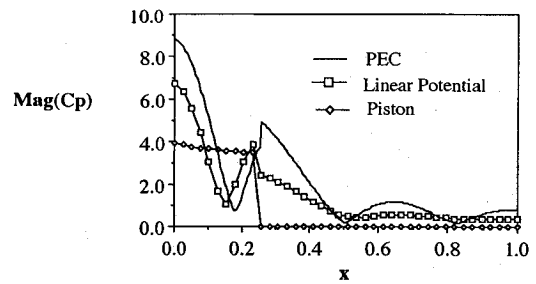
Fig. 14 Oscillating leading-edge flap of a thin-wedge airfoil.

Effect of Frequency

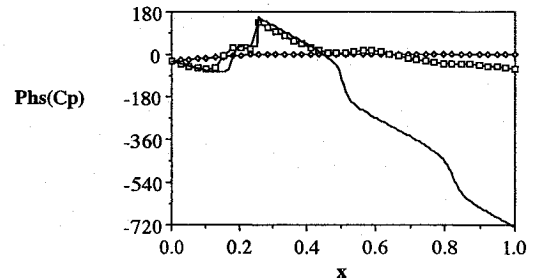
The effect of reduced frequency on the magnitude, Mag , and phase angle, Phs (in units of degrees that are ignored in all figures for simplicity), of the lift and moment coefficients calculated from the present PEC method, piston theory,² and linear theory¹³ are presented in Fig. 13 for an oscillating wedge with a 2-deg semiwedge angle at $M_\infty = 1.2$ and a pitch axis located at the half-chord position. Piston theory provides poor comparisons with the other theories at low reduced frequencies; however, the piston theory solution appears to approach the others at the high-frequency end ($k = 2.0$) in consonance with the condition that $k > 1/M_\infty$ as seen in Fig. 1.

Leading-Edge Flap Oscillation

An oscillating leading-edge flap, with hinge line located at the quarter-chord, of a thin wedge airfoil is shown in Fig. 14. Given the same reduced frequency ($k = 2.0$), two extreme cases in Mach number ($M_\infty = 1.2$ and 99.0) are shown in Figs. 15 and 16. It is seen that both cases produce strong wave interaction according to PEC. Piston theory² underestimates the pressure magnitude on the flap at $M_\infty = 1.2$ and overestimates at $M_\infty = 99.0$. In addition, piston theory fails to predict any pressure changes beyond the hinge line, as expected from its one-dimensionality. Also, large discrepancies in phase angle are found between the results of PEC and those of linear theory¹³ and piston theory, due to the latter theories' exclusion of rotationality and the effects of the wave interaction. In contrast to the waviness in pressure of Fig. 15, the hypersonic wave interaction of Fig. 16 results in a stepwise change in pressure magnitude and phase angle. This is not surprising as the shock is extremely strong

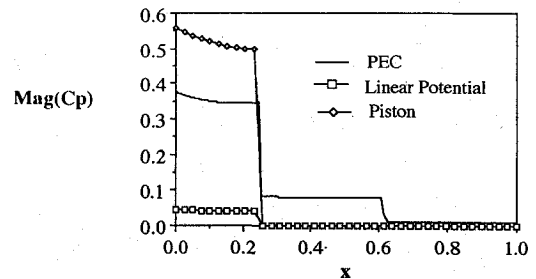


a)

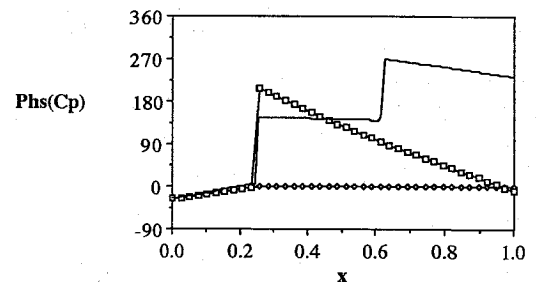


b)

Fig. 15 Comparison of unsteady pressure distribution for an oscillating leading-edge flap at $M_\infty = 1.2$ and $k = 2.0$ with hinge line at the quarter-chord (2-deg semiwedge angle).



a)



b)

Fig. 16 Comparison of unsteady pressure distribution for an oscillating leading-edge flap at $M_\infty = 99.0$ and $k = 2.0$ with hinge line at the quarter-chord (2-deg semiwedge angle).

and nearly coalesced to the wedge surface, whereas the strong Mach wave reflection results in a constant pressure jump in each reflection interval. It is noted that the result for this extreme hypersonic Mach number ($M_\infty = 99$) and $\gamma = 1.0$ serves to illustrate that the present PEC method indeed includes the unsteady Newtonian limit (i.e., $\gamma = 1.0$ and $M_\infty \rightarrow \infty$).

Panel Flutter

Consider the panel flutter model as shown in Fig. 17, where a flexible panel (or membrane) is mounted on the compression side of a wedge surface.

The effect of reduced frequency on the magnitude and phase of the generalized forces calculated from the present PEC method,

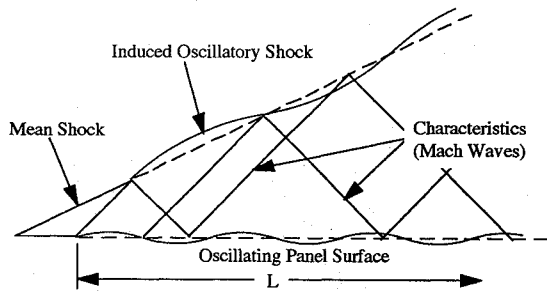


Fig. 17 Panel flutter illustration showing oscillating panels interacting with strong shock wave.

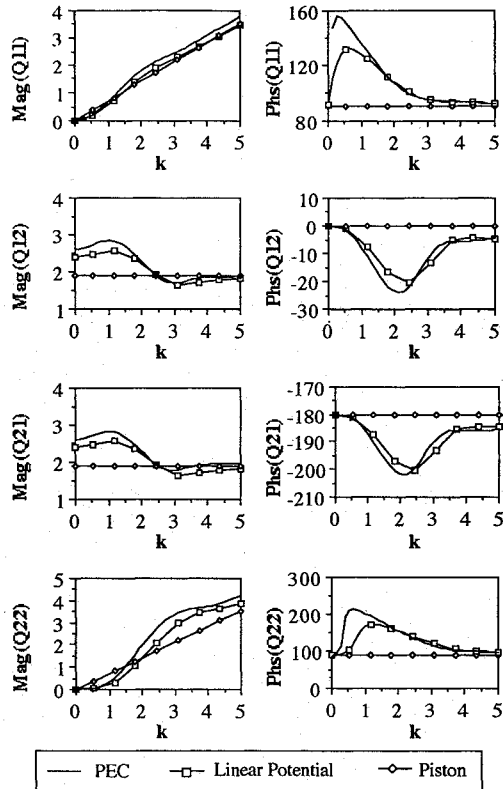


Fig. 18 Effect of frequency on the generalized aerodynamic forces for an oscillating panel ($j = 1$ and 2) at $M_\infty = 1.5$ (2-deg semiwedge angle).

along with piston theory² and linear theory,¹³ is presented in Figs. 18 and 19. The generalized forces are defined as

$$Q_{ij} = \int_0^1 C_{p_i} z_j dx \quad (21)$$

where $z_j = \varepsilon \sin[(j\pi/L)x]e^{ikt}$ is the surface mode shape, and C_{p_i} is the pressure due to the z_i th mode. The results for a 2-deg semiwedge angle and $M_\infty = 1.5$ are shown in Fig. 18. In the present flow region where potential flow is valid, PEC results follow similar trends to that of linear theory in the frequency domain, as expected. Piston theory gives poor results at low and moderate frequencies but appears to give better comparison with the other solutions at the high-frequency end, consistent with Ashley-Landahl's condition $k^2 M^2 \gg 1$. When the Mach number is increased to $M_\infty = 5.0$, Fig. 19 shows small departures between results of PEC and those of piston theory throughout the frequency range of interest, whereas large departures are found in the magnitude of the coupling forces Q_{12} and Q_{21} , which are important factors in determining panel flutter characteristics, computed from linear theory. The finding here, with regards to the piston theory results, is in consonance with Lighthill's postulate $Mk\varepsilon < 1$.

For panel flutter considered at small incidence, caution must be exercised in using the piston theory in the low-to-moderate

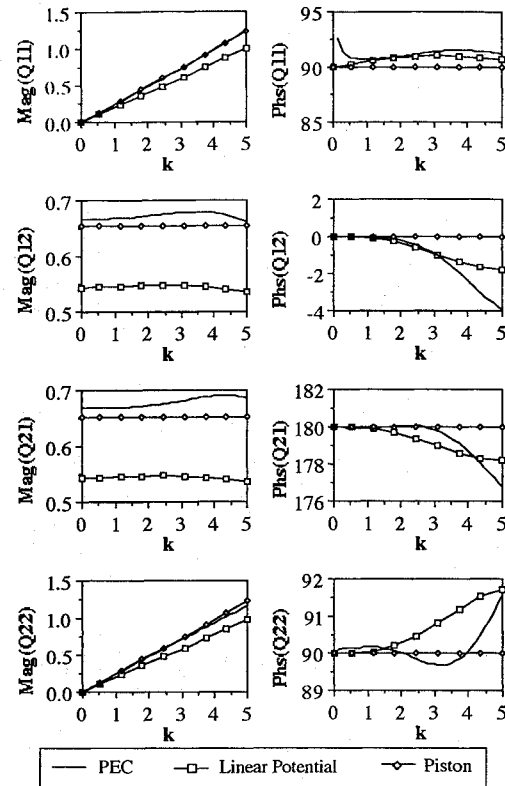


Fig. 19 Effect of frequency on the generalized aerodynamic forces for an oscillating panel ($j = 1$ and 2) at $M_\infty = 5.0$ (2-deg semiwedge angle).

frequency range for low Mach numbers as evident from the discrepancy in the phase angle solution of Fig. 18. Thus, the question of panel flutter boundaries as predicted by PEC, as opposed to those of piston theory and linear theory, deserves further validation with measurement.

Conclusions

A perturbed Euler characteristics (PEC) method has been developed for the treatment of unified hypersonic/supersonic flow over wedge or wedgelike profiles in oscillatory motion and over mounted vibrating panels at small amplitudes. The present PEC method is valid for all Mach numbers ranging from the low-supersonic shock-attached limit to the Newtonian limit and for arbitrary body thickness. Also, the PEC method is completely general in the full-frequency range so long as the motion amplitude is small and the shock remains attached to the body apex. The major thrust of the PEC method is that it can fully account for the effect of unsteady Mach wave/shock wave interaction in the complete range of Mach number and reduced frequency.

For aeroelastic applications, the PEC method is applied to three typical cases. These include rigid wedge in pitching motion, leading-edge flap oscillation, and panel flutter, all including the unsteady Mach wave/shock wave interaction. Unsteady pressures, forces, and moments are presented for all three cases. Computed results are compared with those of Hui's theory, piston theory, and linear (potential) theory. Several observations can be made according to these cases studied.

1) The PEC method accounts fully for the effects of rotationality and unsteady Mach wave/shock wave interaction in the general M - k ranges, as shown in Fig. 1, whereas other methods (Refs. 2, 6, and 8-13) can only account for them partially or regionally.

2) Present studies verify the validity regions for various methods as shown in Fig. 1. In particular, piston theory is found to be restricted by its one-dimensional (hence no upstream influence) and irrotationality characteristics. As a result, piston theory tends to yield nonconservative aeroelastic predictions.

3) Comparison with linear theory results also indicates that the effect of unsteady wave interaction and rotationality are significant at high Mach numbers. However, in the low-to-moderate Mach

number range, linear theory tends to produce conservative trends for aeroelastic predictions.

4) As a prediction tool, piston theory may be acceptable in the moderately high Mach number range; however, caution must be exercised in the low-supersonic and hypersonic Mach number range (e.g., $M = 1.2$ and over 20) where strong wave interaction usually takes place.

Furthermore, the PEC method is extendable to arbitrary profiles and possibly to three-dimensional configurations.

In view of its exactness, in terms of the characteristic formulation for the hyperbolic system, its ease of application, and its effectiveness, the present PEC method should be a promising method for unified hypersonic/supersonic applications to panel flutter and other aeroelastic applications.

References

- ¹Lewis, M. J., Surline, Y., and Anderson, J. D., "An Analytical and Computational Study of Unsteady Shock Motion on Hypersonic Forebodies," AIAA Paper 90-0528, Jan. 1990.
- ²Lighthill, M. J., "Oscillating Airfoils at High Mach Number," *Journal of the Aeronautical Sciences*, Vol. 20, No. 6, 1953, pp. 402-406.
- ³Hayes, W. D., "On Hypersonic Similitude," *Quarterly of Applied Mathematics*, Vol. 5, No. 1, 1947, pp. 105-106.
- ⁴Ashley, H., and Zartarian, G., "Piston Theory—A New Aerodynamic Tool for the Aeroelastician," *Journal of the Aeronautical Sciences*, Vol. 23, No. 12, 1956, pp. 1109-1118.
- ⁵Landahl, M., Mollo-Christensen, E., and Ashley, H., "Parametric Studies of Viscous and Nonviscous Unsteady Flows," ARDC TR 55-13, April 1955.
- ⁶McIntosh, S. C., "Hypersonic Flow over an Oscillating Wedge," *AIAA Journal*, Vol. 3, No. 3, 1965, pp. 433-440.
- ⁷Bailie, J. A., and McFeeley, J. E., "Panel Flutter in Hypersonic Flow," *AIAA Journal*, Vol. 6, No. 2, 1968, pp. 332-337.
- ⁸Carrier, G. F., "On the Stability of the Supersonic Flows Past a Wedge," *Quarterly of Applied Mathematics*, Vol. 6, No. 4, 1949, pp. 367-378.
- ⁹Van Dyke, M. D., "On Supersonic Flow Past an Oscillating Wedge," *Quarterly of Applied Mathematics*, Vol. 11, No. 3, 1953, pp. 360-363.
- ¹⁰Hui, W. H., "Stability of Oscillating Wedges and Carot Wings in Hypersonic and Supersonic Flows," *AIAA Journal*, Vol. 7, No. 8, 1969, pp. 1524-1530.
- ¹¹Hui, W. H., "Interaction of a Strong Shock with Mach Waves in Unsteady Flow," *AIAA Journal*, Vol. 7, No. 8, 1969, pp. 1605-1607.
- ¹²Van Dyke, M. D., "A Study of Hypersonic Small-Disturbance Theory," NACA Rept. 1194, 1954.
- ¹³Liu, D. D., and Pi, W. S., "Transonic Kernel Function Method for Unsteady Transonic Flow Calculations Using a Unified Linear Pressure Panel Procedure," *Proceedings of the AIAA/ASME 21st Fluid and Plasma Dynamics Conference* (Seattle, WA), AIAA, Washington, DC, 1990.